AN ALGEBRAIC SUBSTRUCTURING METHOD FOR LARGE-SCALE EIGENVALUE CALCULATION*

CHAO YANG[†], WEIGUO GAO[‡], ZHAOJUN BAI[§], XIAOYE S. LI[†], LIE-QUAN LEE[¶], PARRY HUSBANDS[†], AND ESMOND NG[†]

Abstract. This paper is concerned with solving large-scale eigenvalue problems by algebraic substructuring. Algebraic substructuring refers to the process of applying matrix reordering and partitioning algorithms to divide a large sparse matrix into smaller submatrices from which a subset of spectral components are extracted and combined to form approximate solutions to the original problem. Through an algebraic analysis, we identify critical conditions under which a simple version of algebraic substructuring works well. This particular version of substructuring is identical to the component mode synthesis (CMS) method (see [R. R. Craig and M. C. C. Bampton, *Coupling of substructures for dynamic analysis*, AIAA J., 6 (1968), pp. 1313–1319] and [W. C. Hurty, *Vibrations of structure systems by component-mode synthesis*, J. Engrg. Mech., 86 (1960), pp. 51–69]) when the matrix reordering is based on a geometric partitioning of the computational domain. We observe an interesting connection between the accuracy of an approximate eigenpair obtained through substructuring and the distribution of the components of eigenvectors of a canonical matrix pencil congruent to the original problem. A priori error bounds for the smallest eigenpair approximation are developed. This development leads to a simple heuristic for choosing spectral components (modes) from each substructure. The effectiveness of such a heuristic is demonstrated with numerical examples. We show that algebraic substructuring can be effectively used to solve a generalized eigenvalue problem arising from the finite element analysis of an accelerator structure.

Key words. algebraic substructuring, projection method, eigenvalue problem

AMS subject classifications. 65F15, 65G05

DOI. 10.1137/040613767

1. Introduction. Substructuring is a commonly used technique for studying the static or dynamic properties of large engineering structures [11, 12, 23, 17]. The basic idea of substructuring is analogous to the concept of domain decomposition, which is widely used in the numerical solution of partial differential equations [28, 25]. By dividing a large structure model or computational domain into a few smaller components (substructures), one can often obtain an approximate solution to the original problem from a linear combination of solutions to similar problems defined on the

substructures. Because solving problems on each substructure requires far less computational power than what would be required to solve the entire problem as a whole, substructuring can lead to a significant reduction in the computational time required to carry out a large-scale simulation and analysis.

The automated multilevel substructuring (AMLS) method [5, 6, 7, 18] is an extension of a substructuring method called *component mode synthesis* (CMS) [11, 17] originally developed in the 1960s. Recent studies have shown that AMLS can be used successfully in the vibration and acoustic analysis of large-scale finite element models of automobile bodies [18, 21]. The frequency response analysis performed in these studies requires computing several thousand eigenvalues and eigenvectors associated with a large-scale symmetric generalized eigenvalue problem. The timing results reported in [18, 21] indicate that AMLS is significantly faster than conventional Lanczos-based approaches [22, 16].

It is important to note that the accuracy achieved by a substructuring method such as AMLS is typically lower than that achieved by the standard Lanczos algorithm. However, in many applications, the level of accuracy required for an approximate solution to an algebraic problem is no more than what is provided by the finite element scheme used to discretize the original continuous problem. Thus, the use of substructuring is easily justified as long as the error associated with the substructuring approximation does not exceed that produced by the finite element discretization.

Asymptotic analysis is performed in [8, 9] to assess the level of accuracy attainable by the CMS method. The analysis is based on the standard finite element theory and properties of the partial differential equation governing the evolution of the structure. The recent work described in [7] provides a high-level mathematical description of the AMLS in a continuous variational setting. However, neither of these studies provides a satisfactory algebraic explanation on why substructuring works well in practice.

Our focus in this paper is on examining substructuring methods for solving large-scale eigenvalue problems from a purely algebraic point of view. We use the term *algebraic substructuring* to refer to the process of applying matrix reordering and partitioning algorithms (such as the *nested dissection* algorithm [15]) to divide a large sparse matrix into smaller submatrices from which a subset of spectral components are extracted and combined to form an approximate solution to the original eigenvalue problem. Through algebraic manipulation, we identify the critical conditions under which a simple version of algebraic substructuring works well. This particular version of substructuring is identical to the CMS method when the matrix reordering is based on the geometric partitioning of the computational domain. We observe an interesting connection between the accuracy of an approximate eigenpair obtained through substructuring and the distribution of components of eigenvectors associated with a canonical matrix pencil congruent to the original problem. An error estimate for the approximation to the smallest eigenpair is developed. The estimate leads to a simple heuristic for choosing spectral components (modes) from each substructure. The effectiveness of such a heuristic is demonstrated with numerical examples. Our analysis is related to but different from the recent work by Bekas and Saad [4], who view algebraic substructuring as an approximation to the spectral Schur complement method [1, 2, 10].

Our interest in algebraic substructuring is motivated in part by an application arising from the simulation of the electromagnetic field associated with the next generation particle accelerator design [20]. We will show through a numerical example that algebraic substructuring can be used effectively to compute the cavity resonance frequencies and the electromagnetic field generated by a linear particle accelerator

model.

Our presentation is organized as follows. In section 2, we give a brief overview of the algorithmic ingredients of a simple algebraic substructuring method. The accuracy of the approximate eigenpairs is analyzed in section 3. Our analysis of algebraic substructuring is confirmed by numerical examples presented in section 4.

Throughout this paper, uppercase and lowercase Latin letters denote matrices and vectors, respectively, while lowercase Greek letters denote scalars. An $n \times n$ identity matrix will be denoted by I_n. The jth column of the identity matrix is denoted by e_j. The transpose of a matrix A is denoted by A^T. We use $\|x\|$ to denote the standard 2-norm of x and use $\|x\|_M$ to denote the M-norm defined by $\|x\|_M = \sqrt{x^T M x}$. We will use $\angle_M(x, y)$ to denote the M inner product induced acute angle (M-angle for short) between x and y. This angle can be computed from

$$\cos \angle_M(x, y) = \frac{x^T M y}{\|x\|_M \|y\|_M}.$$

Similarly, we use $\angle_M(x, \mathcal{S})$ to denote the M-angle between a vector x and a subspace $\mathcal{S}$. This angle can be computed from

$$(1) \qquad \cos \angle_M(x, \mathcal{S}) = \frac{\|Q^T M x\|_2}{\|x\|_M},$$

where Q is an M-orthonormal basis of the subspace $\mathcal{S}$; i.e., $\mathcal{S} = \mathrm{span}\{S\}$ and $Q^T M Q = I$.

A matrix pencil (K, M) is said to be *symmetric definite* if both K and M are symmetric and M is positive definite. A matrix pencil (K, M) is said to be *congruent* to another pencil (A, B) if there exists a nonsingular matrix P such that $A = P^T K P$ and $B = P^T M P$.

2. Algebraic substructuring. In this section, we briefly describe a single-level algebraic substructuring algorithm. Our description does not use any information regarding the geometry or the physical structure on which the original problem is defined.

We are concerned with solving the generalized algebraic eigenvalue problem

$$(2) \qquad Kx = \lambda M x,$$

where K is symmetric and M is symmetric positive definite. We assume both K and M are sparse. They may or may not have the same sparsity pattern. Suppose the rows and columns of K and M have been permuted so that these matrices can be partitioned as

$$(3) \qquad K = \begin{array}{c} \\ n_1 \\ n_2 \\ n_3 \end{array} \begin{array}{ccc} n_1 & n_2 & n_3 \\ \begin{pmatrix} K_{11} & & K_{13} \\ & K_{22} & K_{23} \\ K_{13}^T & K_{23}^T & K_{33} \end{pmatrix} \end{array} \quad \text{and} \quad M = \begin{array}{c} \\ n_1 \\ n_2 \\ n_3 \end{array} \begin{array}{ccc} n_1 & n_2 & n_3 \\ \begin{pmatrix} M_{11} & & M_{13} \\ & M_{22} & M_{23} \\ M_{13}^T & M_{23}^T & M_{33} \end{pmatrix} \end{array},$$

where the labels n_1, n_2, and n_3 are inserted into the top and left borders of the partitioned matrices to indicate the dimension of each submatrix block. The permutation can be accomplished by applying a matrix ordering and partitioning algorithm, such as the nested dissection algorithm [15], to the matrix $|K| + |M|$.

The pencils (K_{11}, M_{11}) and (K_{22}, M_{22}) now define two algebraic substructures that are connected by the third block rows and columns of K and M, which we will refer to collectively as the *interface* block. We assume that n_3 is much smaller than n_1 and n_2.

A single-level algebraic substructuring algorithm proceeds by performing a block factorization

$$(4) \qquad\qquad K = LDL^T,$$

where

$$L = \begin{pmatrix} I_{n_1} & & \\ & I_{n_2} & \\ K_{13}^T K_{11}^{-1} & K_{23}^T K_{22}^{-1} & I_{n_3} \end{pmatrix} \quad \text{and} \quad D = \begin{pmatrix} K_{11} & & \\ & K_{22} & \\ & & \widehat{K}_{33} \end{pmatrix}.$$

The last diagonal block of D, often known as the *Schur complement*, is defined by

$$\widehat{K}_{33} = K_{33} - K_{13}^T K_{11}^{-1} K_{13} - K_{23}^T K_{22}^{-1} K_{23}.$$

The inverse of the lower triangular factor L defines a congruence transformation that, when applied to the matrix pencil (K, M), yields a new matrix pencil $(\widehat{K}, \widehat{M})$:

$$(5) \quad \widehat{K} = L^{-1} K L^{-T} = D \quad \text{and} \quad \widehat{M} = L^{-1} M L^{-T} = \begin{pmatrix} M_{11} & & \widehat{M}_{13} \\ & M_{22} & \widehat{M}_{23} \\ \widehat{M}_{13}^T & \widehat{M}_{23}^T & \widehat{M}_{33} \end{pmatrix}.$$

The off-diagonal blocks of $\widehat{M}$ satisfy

$$\widehat{M}_{i3} = M_{i3} - M_{ii} K_{ii}^{-1} K_{i3} \quad \text{for} \quad i = 1, 2.$$

The last diagonal block of $\widehat{M}$ satisfies

$$\widehat{M}_{33} = M_{33} - \sum_{i=1}^{2} (K_{i3}^T K_{ii}^{-1} M_{i3} + M_{i3}^T K_{ii}^{-1} K_{i3} - K_{i3}^T K_{ii}^{-1} M_{ii} K_{ii}^{-1} K_{i3}).$$

The pencil $(\widehat{K}, \widehat{M})$ is often called the *Craig–Bampton* form [11] in structural engineering. Note that the eigenvalues of $(\widehat{K}, \widehat{M})$ are identical to those of (K, M), and the corresponding eigenvectors $\widehat{x}$ are related to the eigenvectors of the original problem (2) through $\widehat{x} = L^T x$.

The substructuring algorithm constructs a subspace in the form of

$$(6) \qquad\qquad S = \begin{matrix} n_1 \\ n_2 \\ n_3 \end{matrix} \begin{pmatrix} \overset{k_1}{S_1} & \overset{k_2}{} & \overset{n_3}{} \\ & S_2 & \\ & & I_{n_3} \end{pmatrix},$$

where S_1 and S_2 consist of k_1 and k_2 selected eigenvectors of (K_{11}, M_{11}) and (K_{22}, M_{22}), respectively. These eigenvectors will be referred to as *substructure modes* in the discussion that follows. Note that k_1 and k_2 are typically much smaller than n_1 and n_2, respectively.

The approximation to the desired eigenvalues and eigenvectors of the pencil $(\widehat{K}, \widehat{M})$ is obtained by projecting the pencil $(\widehat{K}, \widehat{M})$ onto the subspace spanned by S; i.e., we seek θ and $q \in \mathbb{R}^{k_1+k_2+n_3}$ such that

$$(7) \qquad (S^T \widehat{K} S)q = \theta(S^T \widehat{M} S)q.$$

It follows from the standard Rayleigh–Ritz theory [24, p. 213] that θ serves as an approximation to an eigenvalue of (K, M), and the vector formed by $z = L^{-T}Sq$ is the approximation to the corresponding eigenvector.

A summary of the single-level algebraic substructuring algorithm described in this section is provided below.

ALGORITHM. Single-level algebraic substructuring.

Input: A matrix pencil (K, M), where $K = K^T$ and $M = M^T > 0$;
Output: $\theta_j \in \mathbb{R}$ and $z_j \in \mathbb{R}^n$, $(j = 1, 2, \ldots, k)$ such that $Kz_j \approx \theta_j Mz_j$.

1. Order K and M to be in the form of (3);
2. Perform block factorization $K = LDL^T$;
3. Compute a subset of eigenpairs of the substructures (K_{11}, M_{11}) and (K_{22}, M_{22}). The eigenvectors of each substructure form the columns of S_1 and S_2, respectively;
4. Project the matrix pencil (K, M) into subspace spanned by columns of $Z = L^{-T}S$, where S is defined by (6);
5. Compute k desired eigenpairs (θ_j, q_j) from $(Z^T K Z, Z^T M Z)$, and set $z_j = Zq_j$ $(j = 1, 2, \ldots, k)$; apply the inverse of the permutation used in step 1 to z_j to restore the original order of the solution.

A few remarks are in order.

- Note that the most expensive computational task associated with this algorithm is the block factorization $K = LDL^T$ and the congruence transformation of M required for projecting M into the subspace spanned by $Z = L^{-T}S$. These computational tasks must be carried out with care in order to reduce memory requirements and floating point operations. However, it is beyond the scope of this paper to discuss these important implementation issues.

- Since $k_1 \ll n_1$ and $k_2 \ll n_2$, step 3 of the algorithm can be carried out by using a shift-invert Lanczos algorithm to obtain a small number of desired eigenpairs from each substructure. The cost of this computation is generally small compared to the rest of the computation, especially when this algorithm is extended to a multilevel scheme.

- Similarly, because n_3 is typically much smaller than n_1 and n_2, the dimension of the projected problem (7) is significantly smaller than that of the original problem. Thus, the cost of solving (7) is also small compared to step 2 of the algorithm.

- Decisions must be made on how to select eigenvectors from each substructure. The selection should be made in such a way that the subspace spanned by the columns of Z retains a sufficient amount of spectral information from (K, M). The process of choosing appropriate eigenvectors from each substructure will be referred to as *mode selection*. We will postpone the discussion on this key aspect of the algebraic substructuring algorithm until the next section.

The algebraic substructuring algorithm we presented above becomes identical to the CMS method [11, 17] when the permutation of the pencil in (3) is derived from a

geometric partitioning of the computational domain. The algorithm can be extended in two ways. First, the matrix reordering and partitioning scheme used to create the block structure of (3) can be applied recursively to (K_{11}, M_{11}) and (K_{22}, M_{22}), respectively, to produce a multilevel division of (K, M) into smaller submatrices. The reduced computational cost associated with finding selected eigenpairs from these even smaller submatrices further improves the efficiency of the algorithm. Second, one may replace I_{n_3} in (6) with a subset of eigenvectors of the interface pencil $(\widehat{K}_{33}, \widehat{M}_{33})$. This modification will further reduce the computational cost associated with solving the projected eigenvalue problem (7). A combination of these two extensions yields the AMLS algorithm presented in [18, 7]. However, we will limit the scope of our presentation to a single-level substructuring algorithm.

3. Accuracy and error estimation. Algebraic substructuring allows one to break a large-scale eigenvalue problem into a set of smaller subproblems that are easier to solve. The algorithm would be less attractive to use if one had to compute all eigenvalues and eigenvectors of each subproblem. Fortunately, such a calculation is not necessary, as we will show in this section. In practice, only a small subset of the eigenvectors of (K_{11}, M_{11}) and (K_{22}, M_{22}) is needed to assemble the projection subspace spanned by the columns of the matrix S in (6). To simplify the analysis, we will work with the matrix pencil $(\widehat{K}, \widehat{M})$, where $\widehat{K}$ and $\widehat{M}$ are defined as in (5). As we noted earlier, $(\widehat{K}, \widehat{M})$ and (K, M) have the same set of eigenvalues. If $\widehat{x}$ is an eigenvector of $(\widehat{K}, \widehat{M})$, then $x = L^{-T}\widehat{x}$ is an eigenvector of (K, M), where L is the transformation defined in (4).

Let $(\mu_j^{(i)}, v_j^{(i)})$ be the jth eigenpair of the ith subproblem, i.e.,

$$K_{ii}v_j^{(i)} = \mu_j^{(i)} M_{ii}v_j^{(i)},$$

where $v_j^{(i)}$ is M_{ii}-orthonormal, i.e.,

$$(v_j^{(i)})^T M_{ii} v_k^{(i)} = \begin{cases} 1, & j = k, \\ 0, & \text{otherwise.} \end{cases}$$

To simplify our discussion, we assume that $\mu_j^{(i)}$ has been ordered such that

$$(8) \qquad \mu_1^{(i)} \leq \mu_2^{(i)} \leq \cdots \leq \mu_{n_i}^{(i)}.$$

Let us define $V_i = (v_1^{(i)} v_2^{(i)}, \ldots, v_{n_i}^{(i)})$, $V = \text{diag}(V_1, V_2, I_{n_3})$ and $\Lambda_i = \text{diag}(\mu_1^{(i)}, \mu_2^{(i)}, \ldots, \mu_{n_i}^{(i)})$. An eigenvector of $(\widehat{K}, \widehat{M})$, say $\widehat{x}$, can be expressed as a linear combination of columns of V. That is,

$$(9) \qquad \widehat{x} = Vy = \begin{pmatrix} V_1 & & \\ & V_2 & \\ & & I_{n_3} \end{pmatrix} \begin{pmatrix} y_1 \\ y_2 \\ y_3 \end{pmatrix},$$

where $y = (y_1^T, y_2^T, y_3^T)^T$ is an eigenvector of the generalized eigenvalue problem

$$(10) \qquad \begin{pmatrix} \Lambda_1 & & \\ & \Lambda_2 & \\ & & \widehat{K}_{33} \end{pmatrix} \begin{pmatrix} y_1 \\ y_2 \\ y_3 \end{pmatrix} = \lambda \begin{pmatrix} I_{n_1} & & G_{13} \\ & I_{n_2} & G_{23} \\ G_{13}^T & G_{13}^T & \widehat{M}_{33} \end{pmatrix} \begin{pmatrix} y_1 \\ y_2 \\ y_3 \end{pmatrix},$$

where $G_{13} = V_1^T \widehat{M}_{13}$ and $G_{23} = V_2^T \widehat{M}_{23}$. Note the matrix pencil defined by (10) can be obtained by applying V^T from the left to $\widehat{K}\widehat{x} = \lambda \widehat{M}\widehat{x}$ and expressing $\widehat{x}$ by $\widehat{x} = Vy$. This pencil is clearly congruent to the pencils $(\widehat{K}, \widehat{M})$ and (K, M). Thus they share the same set of eigenvalues. We will refer to (10) as a *canonical form* of the generalized eigenvalue problem (2).

If $\widehat{x}$ can be well approximated by a linear combination of the columns of S, as suggested by the description of the algorithm in section 2, then the vectors y_1 and y_2 must contain only a few large entries. All other components of y_1 and y_2 are likely to be small and negligible. In this section, we seek to formalize this key concept by developing a priori error bounds for the approximations to the smallest eigenvalue of $(\widehat{K}, \widehat{M})$ and the corresponding eigenvector. As we will see below, these bounds can be expressed in terms of the small components of y_1 and y_2.

Suppose $\Lambda_i - \lambda I_{n_i}$ is nonsingular, for $i = 1, 2$. It follows from the first two block rows of the canonical eigenproblem (10) that

$$(11) \qquad y_i = \lambda(\Lambda_i - \lambda I)^{-1} G_{i3} y_3.$$

Consequently, we can express the jth element of y_i by

$$(12) \qquad e_j^T y_i = \frac{\lambda}{\mu_j^{(i)} - \lambda} g_j^{(i)} = \frac{1}{\mu_j^{(i)}/\lambda - 1} g_j^{(i)},$$

where $g_j^{(i)} = e_j^T G_{i3} y_3$. It is easy to see from (12) that, when $|\mu_j^{(i)}/\lambda| \approx 1$, $|e_j^T y_i|$ will be relatively large, provided $|g_j^{(i)}|$ is bounded from below. On the other hand, if $\mu_j^{(i)}$ is far away from λ, and if $|g_j^{(i)}|$ is bounded from above, $|e_j^T y_i|$ will be relatively small. Thus, if λ is surrounded by a few eigenvalues of (K_{ii}, M_{ii}), and if S_i contains only the eigenvectors associated with these eigenvalues, one would expect to obtain an accurate approximation to λ by solving the projected problem (7).

To make the above statements more precise, we introduce some additional notation. Let us define

$$(13) \qquad \rho_k(\omega) = \left| \frac{\lambda_k}{\omega - \lambda_k} \right|,$$

where λ_k is the kth eigenvalue of (K, M). If $|g_j^{(i)}| \in [\gamma_1, \gamma_2]$ for some modest-size constants $\gamma_1 < \gamma_2$, then $\rho_k(\mu_j^{(i)})$ provides a reliable measure for $|e_j^T y_i|$.

It is easy to verify that

$$\rho_k(\mu_{j+1}^{(i)}) \le \rho_k(\mu_j^{(i)}) \quad \text{for } \mu_j^{(i)} > \lambda_k$$

and

$$\rho_k(\mu_j^{(i)}) \le \rho_k(\mu_{j+1}^{(i)}) \quad \text{for } \mu_{j+1}^{(i)} < \lambda_k.$$

These inequalities suggest that $\rho_k(\mu_j^{(i)})$, and therefore $|e_j^T y_i|$, is relatively large when $\mu_j^{(i)}$ is sufficiently close to λ_k.

Let us now focus on the special case in which $k = 1$, i.e., the case associated with the smallest eigenvalue. Because (K_{ii}, M_{ii}) represents the restriction of the pencil $(\widehat{K}, \widehat{M})$ to a subspace, all of its eigenvalues satisfy

$$\lambda_1 \le \mu_j^{(i)} \le \lambda_n.$$

Consequently, the inequality

$$(14) \qquad \rho_1(\mu_1^{(i)}) \geq \rho_1(\mu_2^{(i)}) \geq \cdots \geq \rho_1(\mu_{n_1}^{(i)})$$

holds. Suppose $k_i < n_i$ is the smallest integer such that $\rho_1(\mu_{k_i+1}^{(i)}) \leq \tau$ for some $\tau \ll 1$; then we can assert, under the assumption

$$|g_j^{(i)}| \leq \gamma, \quad \text{for some small constant } \gamma,$$

that $|e_j^T y_i|$ is relatively small for all $j > k_i$. This assertion follows directly from (14) and the observation made in (12). Hence, if our goal is to seek an accurate approximation to λ_1 by projecting $(\widehat{K}, \widehat{M})$ into a subspace $\mathcal{S}$ spanned by the columns of

$$(15) \qquad S = \begin{array}{c} \\ n_1 \\ n_2 \\ n_3 \end{array} \begin{array}{c} \overset{k_1 \quad k_2 \quad n_3}{\begin{pmatrix} S_1 & & \\ & S_2 & \\ & & I_{n_3} \end{pmatrix}}, \end{array}$$

it is natural to set S_i to include only the leading k_i columns of V_i.

Given this choice of subspace, it remains to be shown how much accuracy one can expect from the approximate eigenvalue and eigenvector obtained by applying the Rayleigh–Ritz procedure to S. To simplify our discussion, let us assume that λ_1 is simple. Suppose θ_1 is the smallest eigenvalue of the projected problem

$$(S^T \widehat{K} S)q = \theta(S^T \widehat{M} S)q,$$

and q_1 is the corresponding eigenvector. We will now quantify the accuracy of the *Ritz pair* (θ_1, u_1), where $u_1 = S q_1$, by providing a priori error bounds for both $\theta_1 - \lambda_1$ and $\angle_{\widehat{M}}(\widehat{x}_1, u_1)$ in terms of small elements of y_1 and y_2. Note that $\angle_{\widehat{M}}(\widehat{x}_1, u_1)$ is the $\widehat{M}$-angle (between $\widehat{x}$ and u_1) defined in section 1.

To develop these error bounds, we use the following theorem, which is a generalization of a similar theorem associated with a standard symmetric eigenvalue problem [26, 27].

THEOREM 3.1. *Let* $K, M \in \mathbb{R}^{n \times n}$ *be symmetric matrices and* M *be positive definite. Suppose the eigenpairs of* (K, M), (λ_i, x_i) *have been ordered so that*

$$\lambda_1 < \lambda_2 \leq \cdots \leq \lambda_n.$$

If (θ_i, u_i), $i = 1, 2, \ldots, k$, *are Ritz pairs associated with a* k-*dimensional subspace* $\mathcal{S}$ *ordered so that*

$$\theta_1 \leq \theta_2 \leq \cdots \leq \theta_k,$$

then

$$(16) \qquad \theta_1 - \lambda_1 \leq (\lambda_n - \lambda_1) \sin^2 \angle_M(x_1, \mathcal{S}),$$

$$(17) \qquad \sin \angle_M(u_1, x_1) \leq \sqrt{\frac{\lambda_n - \lambda_1}{\lambda_2 - \lambda_1}} \sin \angle_M(x_1, \mathcal{S}),$$

where $\angle_M(u_1, x_1)$ *denotes the* M-*angle between the vectors* x_1 *and* u_1, *and* $\angle_M(x_1, \mathcal{S})$ *denotes the* M-*angle between* x_1 *and the subspace* $\mathcal{S}$.

The proof of Theorem 3.1 is included in [30]. The theorem suggests that the accuracy of the desired Ritz pair is determined largely by the $\widehat{M}$-angle between the exact eigenvector $\widehat{x}_1$ and the subspace $\mathcal{S}$ from which the Ritz pair is extracted. We now focus on seeking a bound for $\sin \angle_{\widehat{M}}(\widehat{x}_1, \mathcal{S})$. The following theorem, which is a generalization of a similar theorem in [29, p. 250], provides a useful characterization for $\sin \angle_{\widehat{M}}(\widehat{x}_1, \mathcal{S})$.

THEOREM 3.2. *Let x be a vector with $\|x\|_M = 1$ and let $\mathcal{S}$ be a subspace. Then*

$$\sin \angle_M(x, \mathcal{S}) = \min_{w \in \mathcal{S}} \|x - w\|_M.$$

Theorem 3.2 suggests that we can provide a bound for $\sin \angle_{\widehat{M}}(\widehat{x}_1, \mathcal{S})$ by measuring the distance between $\widehat{x}_1$ and a particular choice of a vector $w \in \mathcal{S}$ that is "close" to $\widehat{x}_1$ in the $\widehat{M}$-norm.

Our choice of such a vector $w \in \mathcal{S}$ is made as follows. We define $\hat{y}_i$ $(i = 1, 2)$ by

$$(18) \qquad e_j^T \widehat{y}_i = \begin{cases} e_j^T y_i & \text{for } j \leq k_i, \\ 0 & \text{for } k_i < j \leq n_i, \end{cases}$$

where y_i satisfies

$$(19) \qquad \begin{pmatrix} \Lambda_1 & & \\ & \Lambda_2 & \\ & & \widehat{K}_{33} \end{pmatrix} \begin{pmatrix} y_1 \\ y_2 \\ y_3 \end{pmatrix} = \lambda_1 \begin{pmatrix} I_{n_1} & & G_{13} \\ & I_{n_2} & G_{23} \\ G_{13}^T & G_{23}^T & \widehat{M}_{33} \end{pmatrix} \begin{pmatrix} y_1 \\ y_2 \\ y_3 \end{pmatrix}.$$

It is easy to verify that

$$w = \begin{pmatrix} V_1 & & \\ & V_2 & \\ & & I \end{pmatrix} \begin{pmatrix} \widehat{y}_1 \\ \widehat{y}_2 \\ y_3 \end{pmatrix} \in \mathcal{S} = \text{span}\{S\}.$$

For this particular choice of w, we can easily show that

$$\widehat{x}_1 - w = \begin{pmatrix} V_1 & & \\ & V_2 & \\ & & I \end{pmatrix} \begin{pmatrix} h_1 \\ h_2 \\ 0 \end{pmatrix},$$

where $h_i = y_i - \widehat{y}_i$ for $i = 1, 2$. Consequently, we have

$$\|\widehat{x}_1 - w\|_{\widehat{M}}^2 = (h_1^T \; h_2^T \; 0) \begin{pmatrix} I & & G_{13} \\ & I & G_{23} \\ G_{13}^T & G_{23}^T & \widehat{M}_{33} \end{pmatrix} \begin{pmatrix} h_1 \\ h_2 \\ 0 \end{pmatrix} = h_1^T h_1 + h_2^T h_2.$$

Hence, we can now conclude that

$$(20) \qquad \sin \angle_{\widehat{M}}(\widehat{x}_1, \mathcal{S}) = \min_{w \in \mathcal{S}} \|\widehat{x}_1 - w\|_{\widehat{M}} \leq \sqrt{h_1^T h_1 + h_2^T h_2}.$$

Note that the vector w is essentially obtained from (9) by truncating components associated with the trailing $n_i - k_i$ elements of y_i. These elements are typically small, and they form the nonzero entries of h_i.

Combining (16) and (17) with (20), we obtain the following result.

THEOREM 3.3. *Let $\widehat{K}$ and $\widehat{M}$ be matrices defined in (5). Let $(\lambda_i, \widehat{x}_i)$ $(i = 1, 2, \ldots, n)$ be eigenpairs of the pencil $(\widehat{K}, \widehat{M})$, ordered so that $\lambda_1 < \lambda_2 \leq \cdots \leq \lambda_n$.*

Let (θ_i, u_i) $(i = 1, 2, \ldots, k)$ be the Ritz pairs associated with a k-dimensional subspace $\mathcal{S}$ spanned by the columns of S defined in (15), ordered so that $\theta_1 \leq \theta_2 \leq \cdots \leq \theta_k$. Then

$$\text{(21)} \qquad \theta_1 - \lambda_1 \leq (\lambda_n - \lambda_1)(h_1^T h_1 + h_2^T h_2),$$

$$\text{(22)} \qquad \sin \angle_{\widehat{M}}(u_1, \hat{x}_1) \leq \sqrt{\frac{\lambda_n - \lambda_1}{\lambda_2 - \lambda_1}} \sqrt{h_1^T h_1 + h_2^T h_2},$$

where $h_i = y_i - \widehat{y}_i$, and y_i, $\widehat{y}_i$ $(i = 1, 2)$ are defined by (19) and (18), respectively.

Theorem 3.3 indicates that the accuracy of (θ_1, u_1) is proportional to the size of $h_1^T h_1 + h_2^T h_2$, a quantity that provides a cumulative measure of the "truncated" components in (9). Similar a priori error estimates can be made for other Ritz pairs by utilizing a generalization of Theorems 4.5 and 4.6 in [26, pp. 135–136] which are developed for standard eigenvalue problems. However, to keep our presentation concise, we will not pursue this type of error estimate.

To end this section, we provide an estimate for $h_1^T h_1 + h_2^T h_2$ that is independent of the number of nonzero elements in h_1 and h_2. Note that the nonzero elements of h_i are those elements of y_i associated with

$$\rho_1(\mu_j^{(i)}) < \tau < 1.$$

If $|g_j^{(i)}| \leq \gamma$ for some moderate-size constant γ, then it follows from (12) that each individual element of h_i is either zero or tiny. Moreover, since $\rho_1(\mu_j^{(i)})$ decreases rapidly as $\mu_j^{(i)}$ increases, we can establish a bound for $h_i^T h_i$ in terms of τ under some mild conditions.

To simplify our notation, we will drop the superscript of $\mu_j^{(i)}$ in the following. Suppose the eigenvalues μ_j of (K_{ii}, M_{ii}) are distinct and that

$$\min_{j \geq k_i}(\mu_{j+1} - \mu_j) \geq \delta$$

for some constant $\delta > 0$. Then it is easy to show that

$$
\begin{aligned}
h_i^T h_i &= \sum_{j=k_i+1}^{n_i} (e_j^T h_i)(e_j^T h_i) = \sum_{j=k_i+1}^{n_i} \rho_1^2(\mu_j)(e_j^T G_{i3} y_3)^2 \\
&\leq \left[\sum_{j=k_i+1}^{n_i} \rho_1^2(\mu_j) \right] \gamma^2 \leq \gamma^2 \left[\rho_1^2(\mu_{k_i+1}) + \frac{1}{\delta} \int_{\mu_{k_i+1}}^{\mu_{n_i}} \rho_1^2(\omega) d\omega \right] \\
&= \gamma^2 \left[\frac{\lambda_1}{\mu_{k_i+1} - \lambda_1} \rho_1(\mu_{k_i+1}) + \frac{\lambda_1}{\delta} \left(\frac{\lambda_1}{\mu_{k_i+1} - \lambda_1} - \frac{\lambda_1}{\mu_{n_i} - \lambda_1} \right) \right] \\
\text{(23)} \qquad &\leq \gamma^2 \lambda_1 \left[\frac{1}{\Delta_i} + \frac{1}{\delta} \right] \tau,
\end{aligned}
$$

where $\Delta_i = \mu_{k_i+1} - \lambda_1$. By combining (23) with inequalities (21)–(22) and setting $\Delta = \min\{\Delta_1, \Delta_2, \delta\}$. we obtain

$$\text{(24)} \qquad \frac{\theta_1 - \lambda_1}{\lambda_1} \leq (\lambda_n - \lambda_1)(\alpha \tau),$$

$$\text{(25)} \qquad \sin \angle_{\widehat{M}}(\hat{x}_1, u_1) \leq \sqrt{\lambda_1 \left(\frac{\lambda_n - \lambda_1}{\lambda_2 - \lambda_1} \right)} \sqrt{\alpha \tau},$$

where $\alpha = 4\gamma^2/\Delta$.

We should mention that the presence of multiple (or tightly clustered) eigenvalues of (K_{ii}, M_{ii}) does not alter the qualitative measure of the bounds established in (24) and (25). In that case, we can simply replace the definition of δ with the minimum distances between two adjacent eigenvalue clusters and multiply the bounds by the largest multiplicity of the eigenvalues of (K_{ii}, M_{ii}).

Our assumption that $|g_j^{(i)}|$ is bounded by a moderate constant γ can be justified by noting that

$$(26) \qquad (y_1^T\ y_2^T\ y_3^T) \begin{pmatrix} I & & G_{13} \\ & I & G_{23} \\ G_{13}^T & G_{23}^T & \widehat{M}_{33} \end{pmatrix} \begin{pmatrix} y_1 \\ y_2 \\ y_3 \end{pmatrix} = 1$$

and by the fact that M is positive definite. Since

$$\begin{pmatrix} I & & G_{13} \\ & I & G_{23} \\ G_{13}^T & G_{23}^T & \widehat{M}_{33} \end{pmatrix} = \begin{pmatrix} I & & \\ & I & \\ G_{13}^T & & I \end{pmatrix} \begin{pmatrix} I & & \\ & I & G_{23} \\ & G_{23}^T & \widehat{M}_{33}-G_{13}^T G_{13} \end{pmatrix} \begin{pmatrix} I & & G_{13} \\ & I & \\ & & I \end{pmatrix},$$

it follows from (26) that

$$\|y_1 + G_{13}y_3\| \le 1.$$

Hence, the jth component of $y_1 + G_{13}y_3$ must satisfy

$$(27) \qquad |e_j^T y_1 + g_j^{(1)}| \le 1.$$

It then follows from (27) and (12) that

$$|g_j^{(1)}| \le 1 + |e_j^T y_1| = 1 + \rho_1(\mu_j^{(1)})|g_j^{(1)}|.$$

Consequently,

$$|g_j^{(1)}| \le \frac{1}{1 - \rho(\mu_j^{(1)})} \quad \text{when} \quad \rho(\mu_j^{(1)}) < 1.$$

Thus, if $\rho_1(\mu_j^{(1)}) \ll 1$, then $|g_j^{(1)}|$ is clearly bounded by a small constant. A similar argument can be used to show that $|g_j^{(2)}|$ is bounded by a small constant also.

We should also emphasize that (24) and (25) merely provide a qualitative estimate of the error in the Ritz pair (θ_1, u_1) in terms of the threshold τ that may be used as a heuristic in practice to determine which spectral components of a substructure should be included in the subspace $\mathcal{S}$ defined in (15). This result was verified independently in the recent work by Elssel and Voss [14]. They derived a bound on the relative accuracy of the approximate eigenvalue in a more general setting by making using of the minmax principle for a rational eigenvalue problem.

4. Numerical experiments. We present two numerical examples in this section to illustrate the effectiveness of the single-level algebraic substructuring algorithm presented in section 2. These examples also confirm the analysis carried out in section 3. All experiments are performed in MATLAB. The desired eigenpairs of all pencils are computed by using the MATLAB `eigs` function. For illustration, we computed more eigenvalues and eigenvectors of each subproblem than we actually need in the following experiments. In practice, one would only need to compute a selected number of eigenpairs of (K_{ii}, M_{ii}) incrementally.
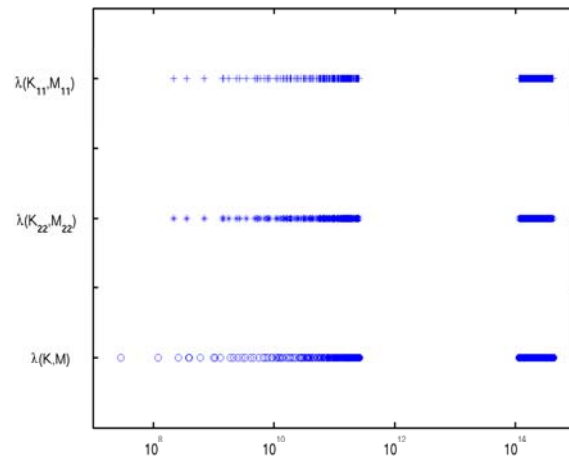
FIG. 1. *The spectra of the pencils* (K_{11}, M_{11}), (K_{22}, M_{22}), *and* (K, M) *associated with the structural dynamics example.*

4.1. Example 1. Structural dynamics. The matrices used in this example, BCSSTK09 and BCSSTM09, are part of the Harwell–Boeing sparse matrix collection [13]. These matrices originated from a dynamic analysis of a clamped plate. The dimensions of these matrices are $n = 1083$. We used METIS [19] to dissect the matrix into two main substructures coupled by a small separator (interface block). The two substructures of the reordered K are identical. The dimension of each substructure is $n_1 = n_2 = 513$. The separator contains only 57 rows and columns. The mass matrix M is diagonal in this example. Applying the same reordering to M does not change its structure.

The spectra of the original matrix pencil (K, M) and the substructure pencils (K_{ii}, M_{ii}) $(i = 1, 2)$ are shown in Figure 1. There is a large gap between the 361st and the 362nd eigenvalues of (K, M). Similar gaps are present in the spectra of (K_{ii}, M_{ii}). In this example, the eigenvalues of interest are the ones on the left side of the spectrum. Naturally, we would select the eigenvectors associated with the smallest eigenvalues of (K_{ii}, M_{ii}) to construct the subspace (6) required in step 5 of the single-level algebraic substructuring algorithm.

To determine how many eigenvectors of (K_{ii}, M_{ii}) we should include in the subspace represented by (6), we examine the ρ-factor defined in (13). It follows from the discussion in section 3 that one may develop a selection scheme by setting a threshold value τ for ρ_1; i.e., one can choose substructure modes that satisfy

$$\rho_1(\mu_j^{(i)}) > \tau$$

for some small τ. However, since the computation of ρ_1 requires the knowledge of the exact λ_1, which we do not have in advance, a more practical scheme is perhaps to compute an approximate ρ-factor by replacing λ_1 in (13) with an approximate eigenvalue σ.

We use $\sigma = \min(\mu_1^{(1)}, \mu_1^{(2)})/2$ in all of our experiments and define

$$(28) \qquad\qquad \widehat{\rho}_1(\omega) = \left| \frac{\sigma}{\omega - \sigma} \right|.$$
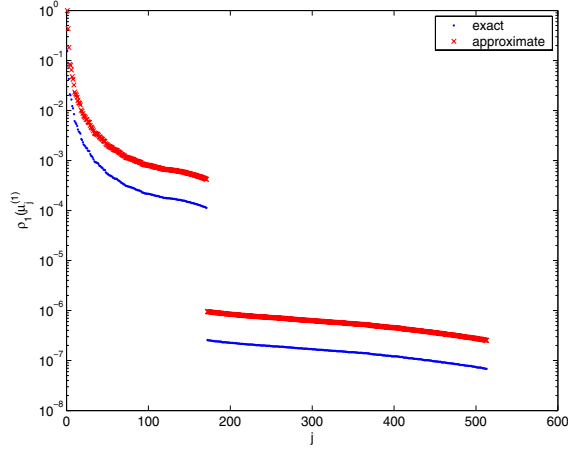
FIG. 2. *The exact (marked by* x*'s) and the approximate (marked by dots) ρ-factors associated with the first substructure of the structural dynamics problem. The exact ρ-factor is defined by (13), and the approximate ρ-factor is defined by (28).*

In Figure 2, we plot both $\rho_1(\mu_j^{(1)})$ and $\widehat{\rho}_1(\mu_j^{(1)})$. (The two substructures in this problem are identical.) The figure clearly shows that there is essentially no qualitative difference between $\rho_1(\mu_j^{(1)})$ and $\widehat{\rho}_1(\mu_j^{(1)})$. Both decrease rapidly as $\mu_j^{(1)}$ increases. There is a clear gap between $\rho_1(\mu_{171}^{(1)})$ and $\rho_1(\mu_{172}^{(1)})$. A similar gap is observed between $\widehat{\rho}_1(\mu_{171}^{(1)})$ and $\widehat{\rho}_1(\mu_{172}^{(1)})$. These gaps reflect the gaps observed in the spectrum of (K_{11}, M_{11}).

Several choices of τ values (listed in Table 1) have been made. The analysis performed in section 3 indicates that, the smaller the value of τ, the more accurate the smallest Ritz pair should be. This prediction is confirmed in Figure 3, where we plot the relative errors of the smallest 50 Ritz values extracted from three subspaces constructed by using these different choices of τ values. Notice that with the choice of $\tau = 10^{-4}$, which corresponds to selecting the leading 171 eigenvectors from each substructure to form the matrix S_i required in (15), θ_1 exhibits roughly 10 digits of accuracy.

TABLE 1
The effect of τ on the number of selected modes associated with the structural dynamics problem, the relative accuracy of the smallest Ritz value, and the relative error bound defined by (21).

τ	k_i	$(\theta_1 - \lambda_1)/\lambda_1$	Relative error bound
10^{-2}	18	1.4×10^{-4}	3.4×10^{0}
10^{-3}	84	2.0×10^{-6}	6.4×10^{-3}
10^{-4}	171	1.2×10^{-12}	4.2×10^{-12}

Even though our error estimate presented in section 3 is targeted only at (θ_1, u_1), Figure 3 shows that the improvement in the accuracy of other Ritz values is also proportional to the decrease of τ.

In this example, the least upper bound for the elements of $g^{(i)}$ used in (12) is roughly $\gamma = 0.28$. Hence, $\rho_1(\mu_j^{(i)})$ provides a reliable upper bound for the magnitude of $e_j^T y_i$ $(i = 1, 2)$, where $(y_1^T, y_2^T, y_3^T)^T$ is the eigenvector associated with the smallest
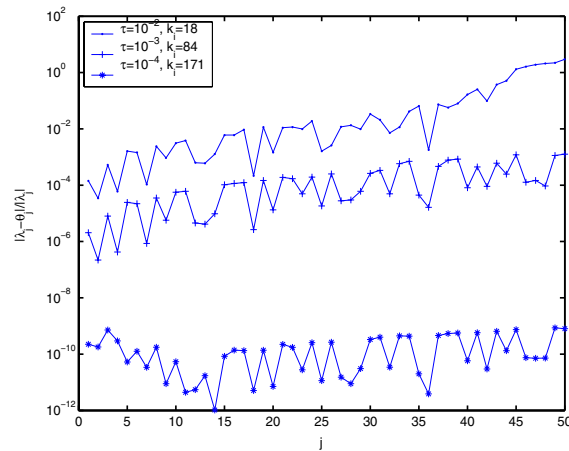
FIG. 3. *The relative error of the smallest* 50 *Ritz values extracted from three subspaces constructed by using different choices of the ρ-factor thresholds (τ values) for the structural dynamics problem.*
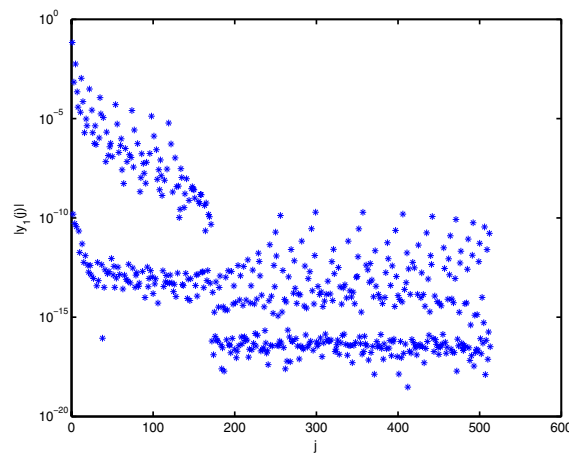
FIG. 4. *The magnitude of $e_j^T y_1$, where $(y_1^T, y_2^T, y_3^T)^T$ is the eigenvector corresponding to the smallest eigenvalue of the canonical problem* (10) *associated with the structural dynamics example.*

eigenvalue (λ_1) of the canonical eigenvalue problem (10).

Judging from the small magnitude of $\rho_1(\mu_j^{(i)})$ for $j > 171$, which is less than 10^{-6}, we predict the magnitude of $e_j^T y_i$, $i = 1, 2$, to be tiny for $j > 171$. This is indeed the case, as is demonstrated in Figure 4, where we plot $|e_j^T y_1|$ (The plot for y_2 is identical.) We observe that $|e_j^T y_1| < 2 \times 10^{-10}$ for all $j > k_1 = 171$. This observation, when used in conjunction with Theorem 3.3, provides a clear explanation for the high accuracy of θ_1 displayed in Figure 3.

Table 1 further illustrates the connections between the mode selection threshold τ, the number of modes selected from each substructure (k_i), the relative accuracy of θ_1, and the error estimates established in Theorem 3.3. Note that the relative error bound listed in the last column of Table 1, which is calculated directly from the right-hand side of (21), tends to be somewhat pessimistic. However, it does provide
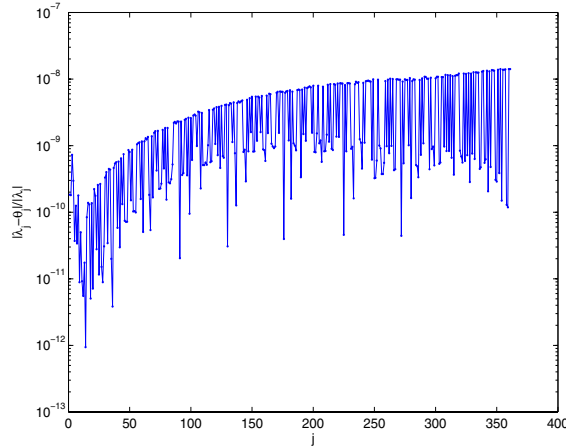
FIG. 5. *The relative error of the smallest* 361 *approximate eigenvalues associated with the structural dynamics problem.*

a qualitative estimate for the relative accuracy of θ_1.

It is interesting to see from Figure 4 that, among the first 171 elements of both y_1 and y_2, many have magnitudes less than 10^{-10}. This observation suggests that one may potentially reduce the dimension of the subspace (6) by excluding eigenvectors of (K_{ii}, M_{ii}) that are associated with these small entries from S_i. We will pursue this idea further in a follow-up paper on mode selection strategies.

We will end this example by pointing out that the large gap between the leading 361 eigenvalues of (K, M) and the rest of the spectrum is a highly favorable feature of this problem. This gap, which also manifests itself in the ρ-factor plots displayed in Figure 2, allows an algebraic substructuring algorithm to easily construct a subspace that contains accurate approximations to the leading 361 eigenvalues of (K, M). Figure 5 shows that, by setting $k_i = 171$, the leading 361 Ritz values extracted from the subspace $\mathcal{S}$ spanned by columns of (15) all have at least 7 digits of accuracy.

4.2. Example 2. Short traveling wave accelerating structure. We show in this example that algebraic substructuring can be used to compute approximate cavity resonance frequencies and the electromagnetic field associated with a small accelerator structure. The matrix pencil used in this example is obtained from a finite element model of a five-cell traveling wave accelerating structure. The three-dimensional geometry of the model is shown in Figure 6. The model contains three cavity cells and two couplers. The dimension of the pencil (K, M) is $n = 1898$. The stiffness matrix K has 336 zero rows and columns. These zero rows and columns are produced by a particular hierarchical vector finite element discretization scheme. Because the null space of K has a special structure, it can be effectively deflated in the algebraic substructuring algorithm. The details of the deflation scheme can be found in [30, 3].

In order to deflate the null space of (K, M) associated with these zero rows and columns, which has no physical significance, we perform the following two-stage matrix reordering:

- A single-level dissection is applied to $|K| + |M|$ first using the METIS [19] software. The dissection produces two substructures of sizes $n_1 = 995$ and $n_2 = 887$, respectively. These substructures are connected by a small separa-
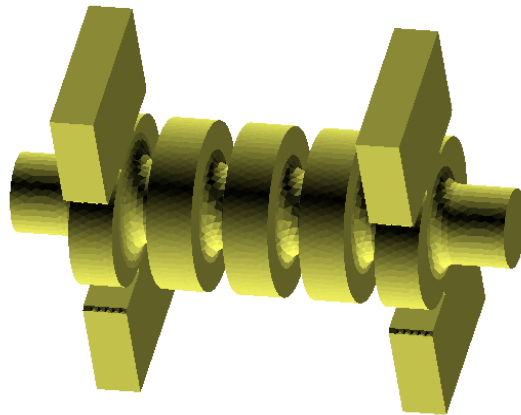
FIG. 6. *The finite element model corresponding to a five-cell traveling wave accelerating structure.*
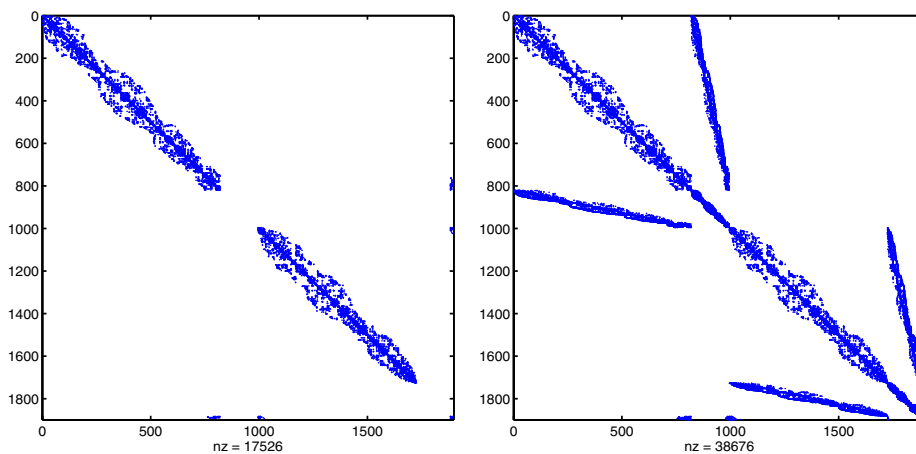
FIG. 7. *The nonzero pattern of the permuted stiffness matrix K (left) and the mass matrix M (right) associated with the traveling wave accelerating structure.*

tor (an interface block) which contains only 16 rows and columns. The K_{11} block of the permuted K contains 175 zero rows and columns, the K_{22} block contains 157 zero rows and columns, and the K_{33} block contains 6 zero rows and columns.

- The nonzero rows and columns of K_{11}, K_{22}, and K_{33} are permuted to the leading blocks of these submatrices. The matrix M is permuted accordingly.

The nonzero patterns of the permuted K and M are displayed in Figure 7. The distribution of the nonzero eigenvalues of (K, M) is shown in Figure 8. We are interested in the smallest nonzero eigenvalues, which appear to be relatively well separated from the large end of the spectrum. In addition to the spectrum of (K, M), we also plot the spectra of (K_{ii}, M_{ii}) $(i = 1, 2)$ in Figure 8. Notice that the spectra of both substructures show a distribution pattern similar to that of (K, M).

In Figure 9 we plot the $\widehat{\rho}$-factors associated with the smallest eigenvalue of the deflated problem. We observe that the $\widehat{\rho}$-factors associated with this example decrease
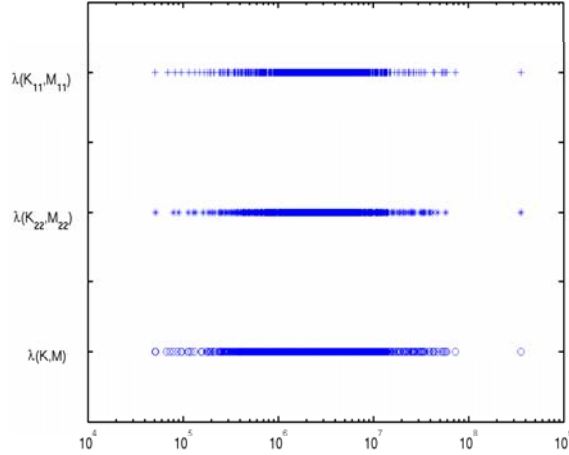
FIG. 8. *The spectra of the pencils* (K_{11}, M_{11}), (K_{22}, M_{22}), *and* (K, M) *associated with the traveling wave accelerating structure.*
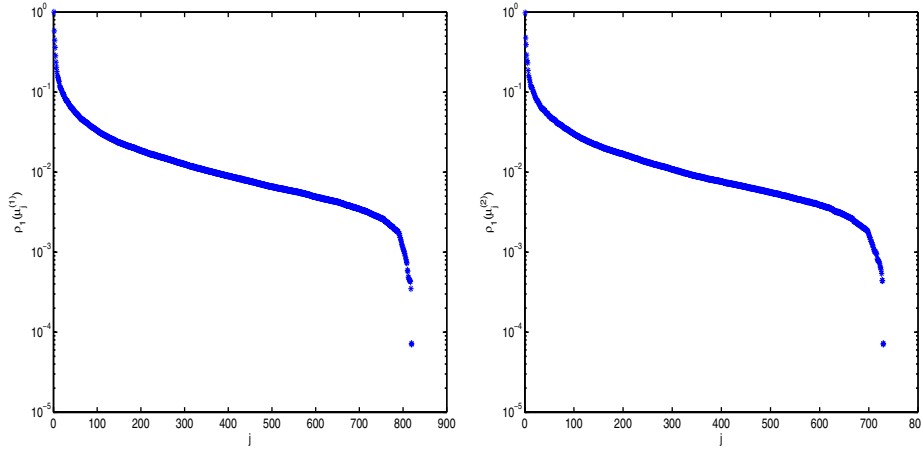
FIG. 9. *The approximate ρ-factors associated with each substructure of the traveling wave accelerating structure.*

at a somewhat slower rate. Three different choices of τ values were used as the thresholds ($\tau = 0.1, 0.05, 0.01$) for selecting substructure modes. The relative accuracy of the 50 smallest nonzero Ritz values extracted from the subspaces constructed with these choices of τ values is displayed in Figure 10.

We observe that with $\tau = 0.1$, θ_1 has roughly four digits of accuracy, which is quite sufficient for this particular discretized model. If we decrease τ down to 0.01, most of the smallest 50 nonzero Ritz values have at least four digits of accuracy.

The least upper bound for $|g_j^{(i)}|$ used in (12) is $\gamma = 0.02$. Thus the ρ-factor gives an overestimate of $|e_j^T y_i|$ in this case. In Figure 11, we plot $|e_j^T y_1|$ and $|e_j^T y_2|$, where $(y_1^T, y_2^T, y_3^T)^T$ is the eigenvector associated with the smallest nonzero eigenvalue of (10). For simplicity, we excluded the values of $|e_j^T y_1|$ and $|e_j^T y_2|$ corresponding to the null space of (K_{11}, M_{11}) and (K_{22}, M_{22}), which have been deflated from our calculations (see section 4). We observe that $|e_j^T y_i|$ is much smaller compared to
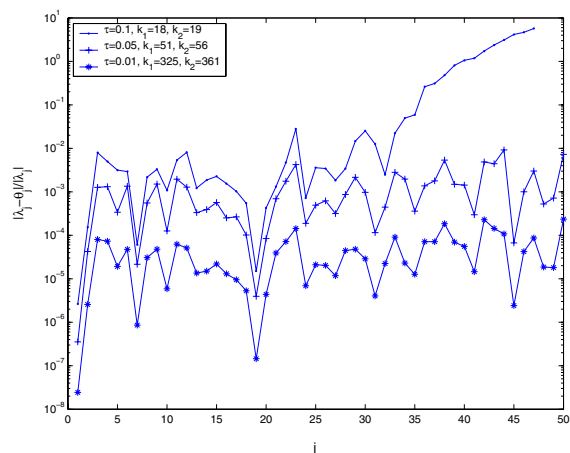
Fig. 10. *The relative error of the smallest* 50 *Ritz values extracted from three subspaces constructed by using different choices of the ρ-factor thresholds (τ values) for the traveling wave accelerating problem.*
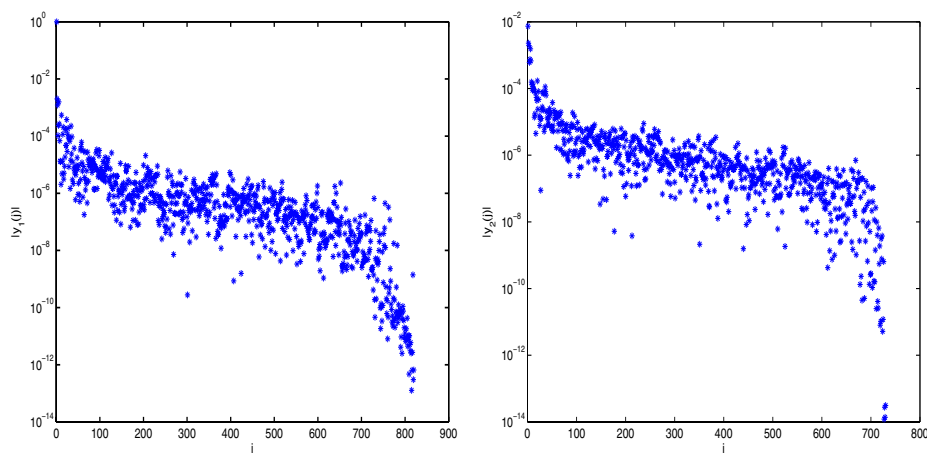
Fig. 11. *The magnitude of $e_j^T y_1$ (left) and $e_j^T y_2$ (right), where $(y_1^T, y_2^T, y_3^T)^T$ is the eigenvector corresponding to the smallest eigenvalue of the canonical problem* (10) *associated with the traveling wave accelerating structure.*

TABLE 2
The effect of τ on the number of selected modes associated with the traveling wave accelerating structure, the relative accuracy of the smallest Ritz value, and the relative error bound defined by (21).

τ	k_1	k_2	$(\theta_1 - \lambda_1)/\lambda_1$	Relative error bound
0.1	18	19	1.4×10^{-4}	1.7×10^{-3}
0.05	51	56	1.2×10^{-5}	2.6×10^{-4}
0.01	325	361	2.4×10^{-8}	2.5×10^{-6}

$\widehat{\rho}_1(\mu_j^{(i)})$, and it decays much faster than the $\widehat{\rho}$-factor also.

We conclude this example by listing in Table 2 the mode selection threshold τ,

the number of modes selected from each substructure (k_i), the relative accuracy of θ_1, and the error estimate computed directly from the right-hand side of (21).

5. Concluding remarks. A purely algebraic analysis of a single-level substructuring algorithm for large-scale eigenvalue calculation is developed in this paper. By applying a sequence of special congruence transformations to (K, M), we transform the original generalized eigenvalue (2) into a canonical problem (10) with a simpler structure. We observed that the desired eigenvector y of the canonical problem (10) often contains only a few large entries. The magnitude of these entries ultimately determines which eigenvectors (modes) of each substructure should be included in the subspace (6), from which approximations to the eigenpairs of (K, M) are extracted. All other substructure modes can essentially be truncated from (9) without sacrificing the required level of accuracy in our approximation. We provided an explicit a priori error estimate for the smallest Ritz pair in terms of the small components of y that are truncated from (9). We also suggested a practical way to estimate the magnitude of each component of y by exploiting its relationship with the "ρ-factor" defined in (13). This estimation leads to a practical way to select substructure modes by specifying a threshold value τ for the ρ-factor. We showed that the accuracy of the smallest Ritz pair is proportional to the size of τ under some mild conditions. A number of numerical examples are provided to confirm our theoretical analysis. Moreover, we demonstrated that an algebraic substructuring algorithm can be an effective tool for computing cavity resonance frequencies and the electromagnetic field generated by a linear accelerator structure.

Our analysis of a simple algebraic substructuring algorithm can be extended to a multilevel setting. Our error estimate can be made for nonextreme Ritz pairs as well. These topics will be pursued in our future research. Another interesting area that would require further research is the development of a better strategy for selecting substructuring modes.

Our presentation has focused on the theoretical aspects of the algebraic substructuring algorithm. Implementation details and comparsion of a multilevel algebraic substructuring algorithm with other methods for large-scale eigenvalue computation will be reported elsewhere.

Acknowledgments. We would like to thank the anonymous referees for their careful reading and helpful comments.

REFERENCES

[1] A. ABRAMOV, *On the separation of the principal part of certain algebraic problems*, Zh. Vychisl. Mat. Mat. i Fiz., 2 (1962), pp. 141–145 (in Russian); USSR Comput. Math. Math. Phys., 1963, pp. 147–151 (in English).

[2] A. ABRAMOV, *Remarks on finding the eigenvalues and eigenvectors of matrices which arise in the application of Ritz's method or in the difference method*, Zh. Vychisl. Mat. i Mat. Fiz., 7 (1962), pp. 644–647 (in Russian); USSR Comput. Math. Math. Phys., 7 (1967), pp. 234–240 (in English).

[3] P. ARBENZ AND Z. DRMAČ, *On positive semidefinite matrices with known null space*, SIAM J. Matrix Anal. Appl., 24 (2002), pp. 132–149.

[4] C. BEKAS AND Y. SAAD, *Computation of Smallest Eigenvalues Using Spectral Schur Complements*, Technical report UMSI-2004-6, Minnesota Supercomputer Institute, University of Minnesota, Minneapolis, MN, 2004.

[5] J. K. BENNIGHOF, *Adaptive multi-level substructuring method for acoustic radiation and scattering from complex structures*, in Computational Methods for Fluid/Structure Interaction, A. J. Kalinowski, ed., AMSE, New York, 1993, pp. 25–38.

[6] J. K. BENNIGHOF AND C. K. KIM, *An adaptive multi-level substructuring method for efficient modeling of complex structures*, in Proceedings of the 33rd AIAA SDM Conference, Dallas, TX, 1992, pp. 1631–1639.

[7] J. K. BENNIGHOF AND R. B. LEHOUCQ, *An automated multilevel substructuring method for eigenspace computation in linear elastodynamics*, SIAM J. Sci. Comput., 25 (2004), pp. 2084–2106.

[8] F. BOURQUIN, *Analysis and comparison of several component mode synthesis methods on one-dimensional domains*, Numer. Math., 58 (1990), pp. 11–34.

[9] F. BOURQUIN, *Component mode synthesis and eigenvalues of second order operators: Discretization and algorithm*, Math. Model. Numer. Anal., 26 (1992), pp. 385–423.

[10] V. S. CHICHOV, *A method for partitioning a high order matrix into blocks in order its eigenvalues*, Zh. Vychisl. Mat. i Mat. Fiz., 1 (1961), pp. 169–173 (in Russian); USSR Comput. Math. Math. Phys., 1962, pp. 186–190 (in English).

[11] R. R. CRAIG AND M. C. C. BAMPTON, *Coupling of substructures for dynamic analysis*, AIAA J., 6 (1968), pp. 1313–1319.

[12] R. R. CRAIG AND C-J. CHANG, *A review of substructure coupling methods for dynamic analysis*, in Advances in Engineering Science, Vol. 2, National Aeronautics and Space Administration, Washington, DC, 1976, pp. 393–408.

[13] I. S. DUFF, R. G. GRIMES, AND J. G. LEWIS, *Users' Guide for the Harwell–Boeing Sparse Matrix Collection (Release 1)*, Technical report RAL-92-086, Rutherford Appleton Laboratory, Oxfordshire, UK, 1992.

[14] K. ELSSEL AND H. VOSS, *An A Priori Bound for Automated Multi-level Substructuring*, Technical report 81, Arbeitsbereich Mathematik, TU Hamburg-Harburg, Germany, 2004.

[15] A. GEORGE, *Nested dissection of a regular finite element mesh*, SIAM J. Numer. Anal., 10 (1973), pp. 345–363.

[16] R. G. GRIMES, J. G. LEWIS, AND H. D. SIMON, *A shifted block Lanczos algorithm for solving sparse symmetric generalized eigenproblems*, SIAM J. Matrix Anal. Appl., 15 (1994), pp. 228–272.

[17] W. C. HURTY, *Vibrations of structure systems by component-mode synthesis*, J. Engrg. Mech., 86 (1960), pp. 51–69.

[18] M. F. KAPLAN, *Implementation of Automated Multilevel Substructuring for Frequency Response Analysis of Structures*, Ph.D. thesis, University of Texas at Austin, Austin, TX, 2001.

[19] G. KARYPIS AND V. KUMAR, METIS—*A Software Package for Partitioning Unstructured Graphs, Partitioning Meshes, and Computing Fill-Reducing Orderings of Sparse Matrices—Version 4.0*, University of Minnesota, Duluth, MN, 1998.

[20] K. KO, N. FOLWELL, L. GE, A. GUETZ, V. IVANOV, L. LEE, Z. LI, I. MALIK, W. MI, C. NG, AND M. WOLF, *Electromagnetic Systems Simulation—from Simulation to Fabrication*, SciDAC report, Stanford Linear Accelerator Center, Menlo Park, CA, 2003.

[21] A. KROPP AND D. HEISERER, *Efficient broadband vibro-acoustic analysis of passenger car bodies using an FE-based component mode synthesis approach*, J. Comput. Acoust., 11 (2003), pp. 139–157.

[22] R. B. LEHOUCQ, D. C. SORENSEN, AND C. YANG, *ARPACK Users' Guide: Solution of Large-Scale Eigenvalue Problems with Implicitly Restarted Arnoldi Methods*, SIAM, Philadelphia, 1998.

[23] R. H. MACNEAL, *Vibrations of Composite Systems*, Technical report OSRTN-55-120, Air Force Office of Scientific Research, Air Research and Development Command, Arlington, VA, 1954.

[24] B. N. PARLETT, *The Symmetric Eigenvalue Problem*, Prentice–Hall, New York, 1980.

[25] A. QUARTERONI AND A. VALLI, *Domain Decomposition Methods for Partial Differential Equations*, Oxford University Press, Oxford, UK, 1999.

[26] Y. SAAD, *Numerical Methods for Large Eigenvalue Problems*, Halsted Press, New York, 1992.

[27] G. L. G. SLEIJPEN, J. VAN DEN ESHOF, AND P. SMIT, *Optimal a priori error bounds for the Rayleigh-Ritz method*, Math. Comp., 72 (2003), pp. 677–684.

[28] B. SMITH, P. BJØRSTAD, AND W. GROPP, *Domain Decomposition*, Cambridge University Press, Cambridge, UK, 1996.

[29] G. W. STEWART, *Matrix Algorithms, Volume* II: *Eigensystems*, SIAM, Philadelphia, 2001.

[30] C. YANG, W. GAO, Z. BAI, X. LI, L. LEE, P. HUSBANDS, AND E. NG, *An Algebraic Substructuring Algorithm for Large-Scale Eigenvalue Calculation*, Technical report LBNL-55055, Lawrence Berkeley National Lab, Berkeley, CA, 2004.